

Crystal structure and luminescence properties of novel $\text{Sr}_{10-x}(\text{SiO}_4)_3(\text{SO}_4)_3\text{O}:x\text{Eu}^{2+}$ phosphor with apatite structure

Qingfeng Guo ^a, Bin Ma ^a, Libing Liao ^{a,*}, Maxim S. Molokeev ^{b,c}, Lefu Mei ^{a,*}, Haikun Liu ^a

^a Beijing Key Laboratory of Materials Utilization of Nonmetallic Minerals and Solid Wastes, National Laboratory of Mineral Materials, School of Materials Sciences and Technology, China University of Geosciences, Beijing 100083, China

^b Laboratory of Crystal Physics, Institute of Physics, SB RAS, Krasnoyarsk 660036, Russia

^c Department of Physics, Far Eastern State Transport University, Khabarovsk 680021, Russia



ARTICLE INFO

Article history:

Received 28 December 2015

Received in revised form

15 April 2016

Accepted 15 April 2016

Available online 16 April 2016

Keywords:

Crystal structure

Apatite

Phosphor

ABSTRACT

In this paper, a series of novel luminescent $\text{Sr}_{10-x}(\text{SiO}_4)_3(\text{SO}_4)_3\text{O}:x\text{Eu}^{2+}$ phosphors with apatite structure were synthesized by a high temperature solid-state reaction. The phase structure, photoluminescence (PL) properties, as well as the PL thermal stability were investigated. $\text{Sr}_{9.92}(\text{SiO}_4)_3(\text{SO}_4)_3\text{O}:0.08\text{Eu}^{2+}$ phosphor exhibits better thermal quenching resistance, retaining the luminance of 66.55% at 150 °C compared with that at 25 °C. The quenching concentration of Eu^{2+} in $\text{Sr}_{10}(\text{SiO}_4)_3(\text{SO}_4)_3\text{O}$ was about 0.08 (mol) with the dipole-quadrupole interaction. The $\text{Sr}_{10-x}(\text{SiO}_4)_3(\text{SO}_4)_3\text{O}:x\text{Eu}^{2+}$ phosphors exhibited a broad-band green emission at 538 nm upon excitation at 396 nm. The results indicate that $\text{Sr}_{10-x}(\text{SiO}_4)_3(\text{SO}_4)_3\text{O}:x\text{Eu}^{2+}$ phosphors have potential applications as near UV-convertible phosphors for white-light UV LEDs.

© 2016 Elsevier Ltd and Techna Group S.r.l. All rights reserved.

1. Introduction

As we know, white light emitting diodes (w-LEDs) solid-state lighting technology has been widely used and attracted lots of research interests due to their promising features, such as low power consumption, high efficiency, as well as environmental friendliness characteristics [1–4]. In general, the typical w-LEDs can be obtained by a combination of a yellow-emitting $\text{Y}_3\text{Al}_5\text{O}_{12}:\text{Ce}^{3+}$ phosphor and a blue InGaN chip [5]. However, these phosphors are suffering from some disadvantages such as poor color-rendering index and high correlated color temperature caused by the weak red emission. Therefore, it is necessary to introduce bright tricolor (red, green, and blue) phosphors for the development of tricolor emission phosphors upon *n*-UV light (350–420 nm) [6,7]. It is known to us that the rare earth ions plays an important and irreplaceable role in lighting and display fields for their $4f \rightarrow 4f$ or $5d \rightarrow 4f$ transitions. As a highly efficient activator, Eu^{2+} has a wide range of emission ascribed to the allowed $4f^65d^1 \rightarrow 4f^7$ transitions, which has been widely investigated in many compounds, such as $\text{Sr}_5(\text{PO}_4)_3\text{Cl}:\text{Eu}^{2+}$ [8], $\text{BaMgAl}_{10}\text{O}_{17}:\text{Eu}^{2+}$ [9], $\text{Ca}_3\text{Si}_2\text{O}_7:\text{Eu}^{2+}$ [10]. Thus, it is necessary to find new hosts with a specific crystal field to accommodate Eu^{2+} ions.

Alternatively, compounds with apatite structure have attracted

many attentions due to their excellent stability and compatibility with efficient luminescent in *n*-UV LEDs. Therefore, many apatite structure type phosphors for w-LEDs application have been widely developed, such as $\text{Ca}_9\text{Mg}(\text{PO}_4)_6\text{F}_2:\text{Eu}^{2+}$, Mn^{2+} [11], $\text{Ca}_2\text{Gd}_8(\text{SiO}_4)_6\text{O}_2:\text{Eu}^{3+}$ [12], $\text{Ca}_4\text{Y}_6(\text{SiO}_4)_6\text{O}:\text{Ce}^{3+}/\text{Mn}^{2+}/\text{Tb}^{3+}$, [13], and $\text{Na}_6(\text{SO}_4)_2\text{FCl}:\text{RE}$ [14]. To the best of our knowledge, the $\text{Sr}_{10}(\text{SiO}_4)_3(\text{SO}_4)_3\text{O}:\text{Eu}^{2+}$ phosphor has not been reported up to now.

In the present work, we successfully synthesized $\text{Sr}_{10-x}(\text{SiO}_4)_3(\text{SO}_4)_3\text{O}:x\text{Eu}^{2+}$ phosphors with apatite structure for the first time. The relationship between the crystal structure and the luminescence properties of Eu^{2+} in $\text{Sr}_{10}(\text{SiO}_4)_3(\text{SO}_4)_3\text{O}$ (SSSO) host was investigated in detail. Results show that the SSSO:Eu²⁺ phosphors can be potentially applied as the green-emitting component in w-LEDs.

2. Experimental procedure

2.1. Materials and synthesis

SSSO:Eu²⁺ phosphors were synthesized by a traditional high temperature solid-state reaction method. Stoichiometric amounts of raw materials SrCO_3 (Aldrich, 99.9%), SiO_2 (Aldrich, 99.9%), SrSO_4 (Aldrich, 99.9%) and Eu_2O_3 (A.R.) were weighed and mixed by grinding in an agate mortar. The mixture was firstly pre-heated at 650 °C for 3 h in air atmosphere in alumina crucibles. After the preliminary products were ground thoroughly in an agate mortar

* Corresponding authors.

E-mail addresses: clay@cugb.edu.cn (L. Liao), mlf@cugb.edu.cn (L. Mei).

after cooling to room temperature, they were placed into alumina crucibles and annealed at 1150 °C in a reducing atmosphere in flowing gas (10% H₂+90% N₂) for 5 h. After firing, the samples were gradually cooled to room temperature in the furnace. The products were crushed and finally obtained for measurements.

2.2. Characterization methods

The phase structures of the as-prepared samples were checked by X-ray powder diffractometer (D/max-rA 12kw, Japan) with Cu K α radiation ($\lambda=1.5418\text{ \AA}$) from 4° to 70° (2 θ). The step scanning rate (2 θ values ranging from 10 to 120°) used for Rietveld analysis was 2 s/step with a step size of 0.02°. Rietveld refinement of the structure of the select Sr_{9.92}(SiO₄)₃(SO₄)₃O:0.08Eu²⁺ was performed by using the computer software TOPAS [15]. Room temperature photoluminescence excitation (PLE) and emission (PL) spectra were measured on a fluorescence spectrophotometer (F-4600, HITACHI, Japan) with a photomultiplier tube operating at 400 V, and a 150 W Xe lamp was used as the excitation lamp. Besides, the temperature-dependence luminescence properties were measured on the same spectrophotometer combined with a self-made heating attachment and a computer-controlled electric furnace.

3. Results and discussion

3.1. Phase purity and structure

The XRD patterns of the standard Sr₁₀(PO₄)₆O (ICSD no. 168209) [16] and Sr_{10-x}(SiO₄)₃(SO₄)₃O:xEu²⁺ ($x=0.002, 0.04, 0.06, 0.08$, and 0.10) samples are shown in Fig. 1. It is obvious that the XRD patterns of all the Sr_{10-x}(SiO₄)₃(SO₄)₃O:xEu²⁺ phosphors can be exactly assigned to the phase of Sr₁₀(PO₄)₆O (ICSD no. 168209), belonging to hexagonal structure with the group space $P6_3/m$, and no second phases is observed. Thus, doping of Eu²⁺ does not cause any detectable change in the crystal lattice. As we know, Sr²⁺ ions have two different coordination numbers (CN) in the structure of SSSO. Sr1 is defined as being nine-fold coordinated, and Sr2 is defined as being seven-fold coordinated. The effective ionic radii of Eu²⁺ ($r=1.20\text{ \AA}$ for CN=7 and $r=1.30\text{ \AA}$ for CN=9) is the close to that of Sr²⁺ ($r=1.21\text{ \AA}$ for CN=7 and $r=1.31\text{ \AA}$ for CN=9) [17]. Therefore, we suggest that the activators Eu²⁺ ions are expected to occupy the Sr²⁺ sites randomly in the SSSO

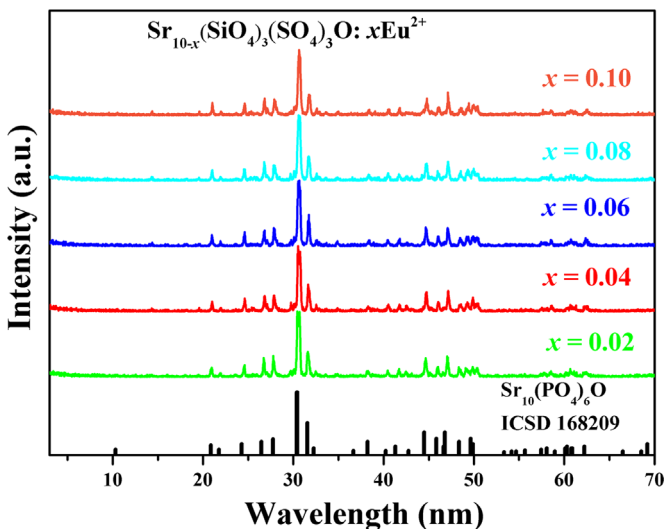


Fig. 1. The XRD patterns of Sr_{10-x}(SiO₄)₃(SO₄)₃O:xEu²⁺ ($x=0.002, 0.04, 0.06, 0.08$, and 0.10), and the standard data for Sr₁₀(PO₄)₆O (ICSD card no. 168209) is shown as a reference.

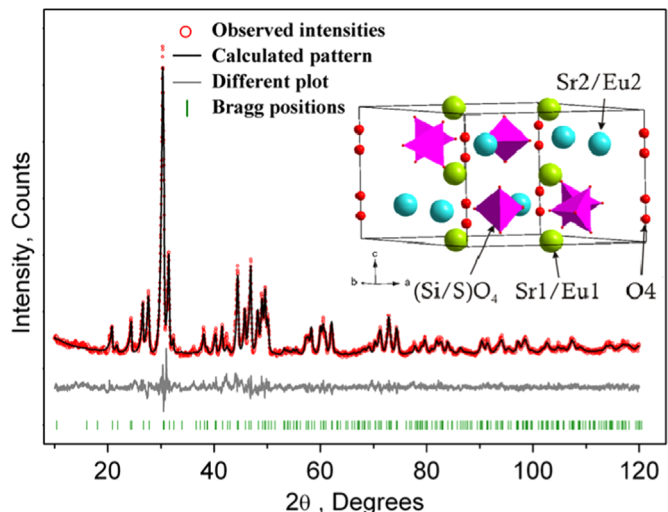


Fig. 2. Rietveld analysis patterns for X-ray powder diffraction data of Sr_{9.92}(SiO₄)₃(SO₄)₃O:0.08Eu²⁺. The solid black lines are calculated intensities, and the red dots are the observed intensities. The gray solid lines below the profiles stand for the difference between the observed and calculated intensities. The short green vertical lines show the position of Bragg reflections of the calculated pattern, and the inset of this figure shows the crystal Structure of Sr₁₀(SiO₄)₃(SO₄)₃O compound. (For interpretation of the references to color in this figure legend, the reader is referred to the web version of this article.)

host. To better understand the crystallographic sites of Eu²⁺ in SSSO, the powder diffraction data of Sr_{9.92}(SiO₄)₃(SO₄)₃O:0.08Eu²⁺ was collected at room temperature for Rietveld analysis. Rietveld refinement was performed by using TOPAS 4.2. Almost all peaks were indexed by hexagonal cell ($P6_3/m$) with parameters close to Sr₁₀(PO₄)₆O (apatite-type structure). Therefore crystal structure of Sr₁₀(PO₄)₆O was taken as starting model for Rietveld refinement. The inset of Fig. 2 illustrates the structure of SSSO compound. As given in the inset of Fig. 2, The P atoms are tetrahedrally coordinated forming [SiO₄] or [SO₄] groups, which are isolated from each other. There are two independent sites for Sr²⁺ ions in the structure and both of them were occupied by Eu²⁺ ion with fixed occupancy $p=0.08$ and Sr ion with $p=0.992$. One P site in an asymmetric unit was occupied by Si and S ions with $p=0.5$, respectively, according to suggested formula. Refinement was stable and gives low R -factors (Table 1, Fig. 2). The reliability parameters of refinement are $R_{wp}=9.37\%$, $R_p=7.04\%$, and GOF=2.42, which can verify the phase purity of the as-prepared sample. Fractional atomic coordinates and isotropic displacement parameters (\AA^2) of Sr_{9.92}(SiO₄)₃(SO₄)₃O:0.08Eu²⁺ is shown in Table 2. Besides, the small refined residual factors indicate that Eu²⁺ can occupy both types of Sr²⁺ sites with seven- or nine-fold coordination randomly.

Table 1
Main parameters of processing and refinement of the Sr_{9.92}(SiO₄)₃(SO₄)₃O:0.08Eu²⁺.

Compound	Sr _{9.92} (SiO ₄) ₃ (SO ₄) ₃ O:0.08Eu ²⁺
Space group	$P6_3/m$
$a, \text{\AA}$	9.8103(7)
$c, \text{\AA}$	7.2593(6)
$V, \text{\AA}^3$	605.0(1)
2 θ -interval, °	10–120
No. of reflections	332
No. of refined parameters	46
$R_{wp}, \%$	9.37
$R_p, \%$	7.04
$R_{exp}, \%$	3.88
χ^2	2.42
$R_B, \%$	2.85

Table 2

Fractional atomic coordinates and isotropic displacement parameters (\AA^2) of $\text{Sr}_{9.92}(\text{SiO}_4)_3(\text{SO}_4)_3\text{O}:0.08\text{Eu}^{2+}$.

	x	y	z	Biso	Occ.
Sr1	1/3	2/3	-0.0009 (9)	0.9 (2)	0.992
Eu1	1/3	2/3	-0.0009 (9)	0.9 (2)	0.008
Sr2	0.0112 (5)	0.2488 (3)	0.25	1.1 (1)	0.992
Eu2	0.0112 (5)	0.2488 (3)	0.25	1.1 (1)	0.008
Si	0.4090 (9)	0.3753 (8)	0.25	0.4 (2)	0.5
S	0.4090 (9)	0.3753 (8)	0.25	0.4 (2)	0.5
O1	0.326 (2)	0.490 (2)	0.25	1.5 (3)	1
O2	0.598 (2)	0.475 (2)	0.25	1.5 (3)	1
O3	0.350 (1)	0.278 (1)	0.087 (2)	1.5 (3)	1
O4	0	0	0.170 (6)	1.5 (3)	0.25

3.2. Luminescence properties

The representative photoluminescence excitation (PLE) and photoluminescence (PL) spectra of the as-prepared $\text{Sr}_{9.92}(\text{SiO}_4)_3(\text{SO}_4)_3\text{O}:0.08\text{Eu}^{2+}$ phosphor are presented in Fig. 2. The PLE spectrum of the phosphor shows a broad absorption centered at 396 nm ranging from 250 to 525 nm, which is attributed to the $4f$ - $5d$ transitions of the doped Eu^{2+} ions. Under the excitation at 396 nm, the PL spectrum exhibits a green emission band peaked at 538 nm. In addition, the PL spectrum can be divided into two dotted bands centered at about 529 and 555 nm by using Gaussian fitting, as shown in Fig. 3. Based on the earlier discussion by Van Uitert, the emission position of Eu^{2+} ions is strongly dependent on its local crystal environment, which is suggested to obey the following equation: [18,19]

$$E = Q \left[1 - \left(\frac{V}{4} \right)^{\frac{1}{V}} 10^{-\frac{n \times Ea \times r}{80}} \right] \quad (1)$$

Where E represents the position of the rare-earth ion emission peak (cm^{-1}), Q is the energy position of the lower d-band edge for the free ions ($34,000 \text{ cm}^{-1}$ for Eu^{2+}), V stands for the valence of the “active” cation ($V=2$ for Eu^{2+}), n is the number of anions in the immediate shell around the “active” cation, r is the effective radius of the host cations (Sr^{2+}) replaced by the Eu^{2+} ion (\AA), and Ea is the electron affinity of the atoms that form anions, which is constant in the same host. The effective ionic radius of Sr^{2+} with nine-coordination is bigger than that with seven-coordination. Thus, we proposed that the emission peaks centered at 529 and 555 nm are attributed to Eu^{2+} ions with nine-coordination and seven-coordination, respectively.

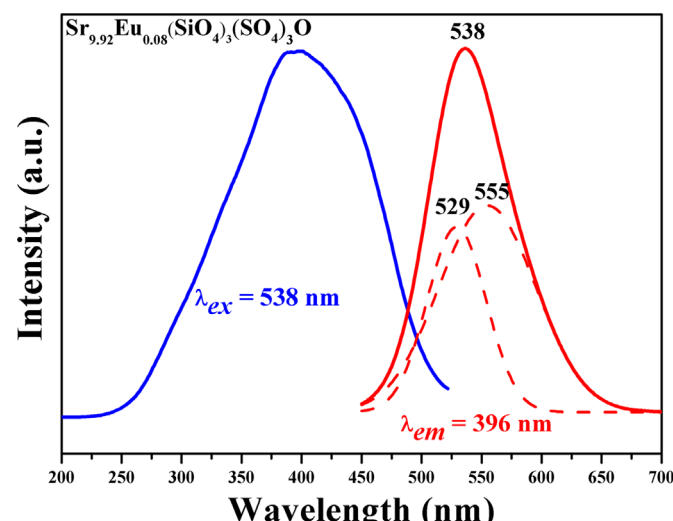


Fig. 3. PLE (left) and PL (right) spectrum of the selected $\text{Sr}_{9.92}(\text{SiO}_4)_3(\text{SO}_4)_3\text{O}:0.08\text{Eu}^{2+}$ fitted by Gaussian.

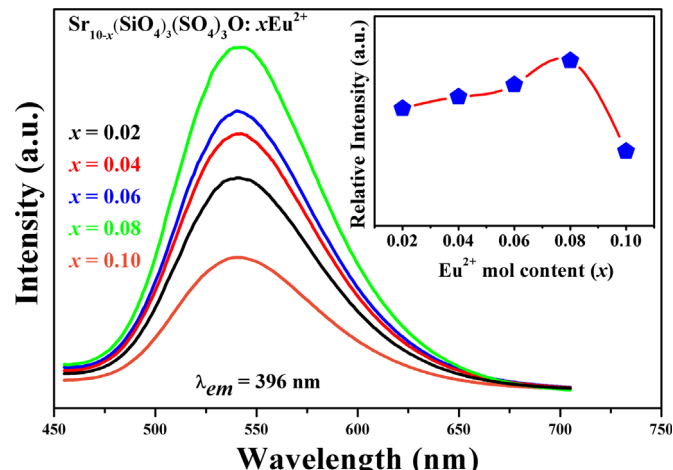


Fig. 4. The PL spectra of $\text{Sr}_{10-x}(\text{SiO}_4)_3(\text{SO}_4)_3\text{O}:x\text{Eu}^{2+}$ ($x=0.002, 0.04, 0.06, 0.08$, and 0.10) phosphors under 396 nm excitation, and the inset of this figure shows the Eu^{2+} doping concentration dependent PL intensity. (For interpretation of the references to color in this figure legend, the reader is referred to the web version of this article.)

Fig. 4 displays the PL spectra of $\text{Sr}_{10-x}(\text{SiO}_4)_3(\text{SO}_4)_3\text{O}:x\text{Eu}^{2+}$ phosphors ($x=0.002, 0.04, 0.06, 0.08$, and 0.10) under 396 nm light excitation, and the inset of Fig. 4 shows the Eu^{2+} doping concentration dependent PL intensity. The result displayed that the optimal doping concentration of Eu^{2+} in SSSO host was 0.08 mol . It can be easily seen that the PL intensity would decrease when the concentration exceeds the critical concentration, which is caused by the concentration quenching effect. Moreover, the critical energy transfer distance R_c between Eu^{2+} ions can be estimated by using concentration quench equation proposed by Blasse: [20,21]

$$R_c \approx 2 \left[\frac{3V}{4\pi x_c N} \right]^{1/3} \quad (2)$$

Where V stands for the volume of the unit cell, x_c is the atom fraction of activator at which the quenching occurs, and N represents the number of host cations in the unit cell. For the SSSO host, $N=10$, V is estimated to be 605.01 \AA^3 , x_c is 0.08 for emission peak at 538 nm . The critical distances R_c of energy transfer can be estimated to be about 10.41 \AA ($x_c=0.08$) using Eq. (2). Furthermore, the non-radiative transitions between Eu^{2+} ions took place via electric multipolar interactions with R_c more than 5 \AA according to the Dexter theory. Moreover, the interaction type between sensitizers or between sensitizer and activator can be calculated by the following equation: [22,23]

$$\frac{I}{x} = K [1 + \beta(x)^{\frac{\theta}{3}}]^{-1} \quad (3)$$

where I is the emission intensity, x stands for the activator concentration, K and β are constants for each type of interaction for a given host lattice, and θ is an indication of electric multipolar character. In general, $\theta=6, 8, 10$ can be assigned to dipole-dipole ($d-d$), dipole-quadrupole ($d-q$), quadrupole-quadrupole ($q-q$) interactions, respectively. Fig. 5 illustrates the fitting line of $\log(I/x)$ vs. $\log(x)$ in $\text{Sr}_{10-x}(\text{SiO}_4)_3(\text{SO}_4)_3\text{O}:x\text{Eu}^{2+}$ phosphors for the emission peak of 538 nm beyond the quenching concentration. The fitting line was found to be relatively linear with a slope equal to $-\theta/3$, and the slope was determined to be -1.447 . Therefore, the value of θ can be calculated to be 4.341. In this case, dipole-dipole interactions play the dominant role for concentration quenching of Eu^{2+} ions in $\text{Sr}_{10-x}(\text{SiO}_4)_3(\text{SO}_4)_3\text{O}:x\text{Eu}^{2+}$ phosphors.

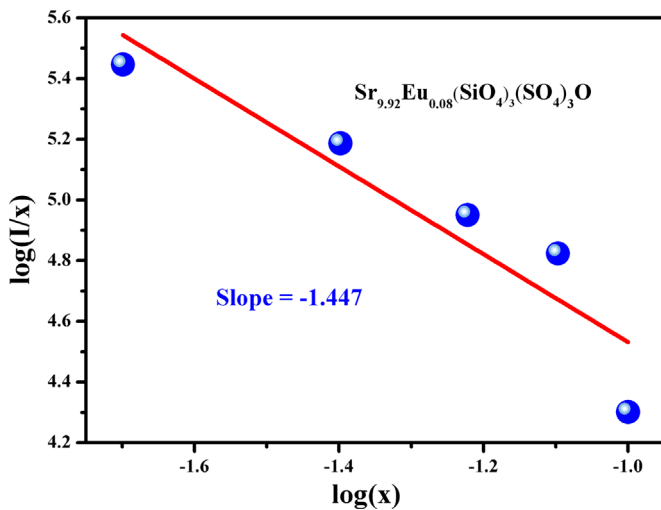


Fig. 5. The fitting line of $\log(I/x)$ vs. $\log(x)$ in $\text{Sr}_{9.92}(\text{SiO}_4)_3(\text{SO}_4)_3\text{O}:0.08\text{Eu}^{2+}$ phosphor beyond the quenching concentration.

The thermally stable luminescence properties of $\text{Sr}_{9.92}(\text{SiO}_4)_3(\text{SO}_4)_3\text{O}:0.08\text{Eu}^{2+}$ phosphor has been monitored by 396 nm from 25 °C to 250 °C, and the temperature dependence PL spectra of $\text{Sr}_{9.92}(\text{SiO}_4)_3(\text{SO}_4)_3\text{O}:0.08\text{Eu}^{2+}$ sample are shown in Fig. 6(a) and (b), respectively. The emission intensities of the sample decrease gradually with the temperature increases, and $\text{Sr}_{9.92}(\text{SiO}_4)_3(\text{SO}_4)_3\text{O}:0.08\text{Eu}^{2+}$ phosphor seems to possess good thermal stability. Besides, the emission wavelength shows slight blue shift from 538 to 530 nm with raising temperature, which was caused by the thermally active phonon-assisted excitation from the lower-energy emission band to the higher-energy emission band in the excited states of Eu^{2+} [24]. The PL intensity of $\text{Sr}_{9.97}(\text{PO}_4)_6\text{O}:0.03\text{Eu}^{2+}$ drops to 66.55% when the temperature is raised to 150 °C compared with that of 25 °C.

In order to give a quantitative analysis on the thermal stable luminescence behavior of $\text{Sr}_{9.92}(\text{SiO}_4)_3(\text{SO}_4)_3\text{O}:0.08\text{Eu}^{2+}$ phosphor, the Arrhenius equation were employed to calculate the activation energy as following: [25,26]

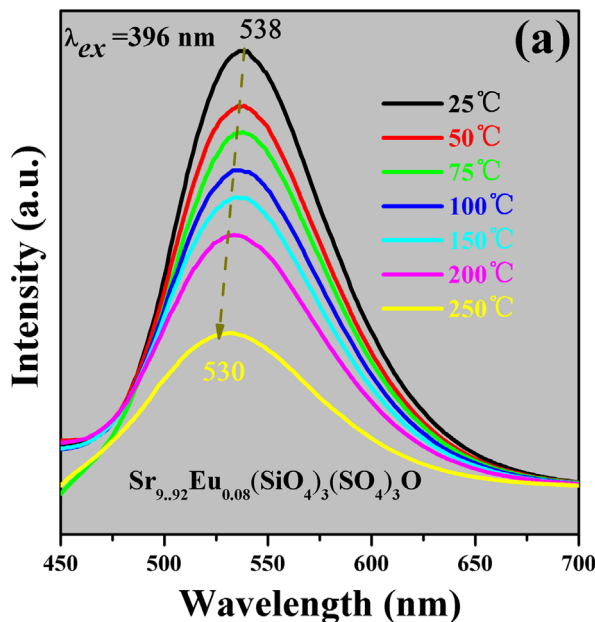


Fig. 6. The PL spectra ($\lambda_{\text{ex}}=396 \text{ nm}$) of $\text{Sr}_{9.92}(\text{SiO}_4)_3(\text{SO}_4)_3\text{O}:0.08\text{Eu}^{2+}$ phosphor under different temperatures in the range of 25–250 °C (a), and the relative emission intensities as a function of temperature (b).

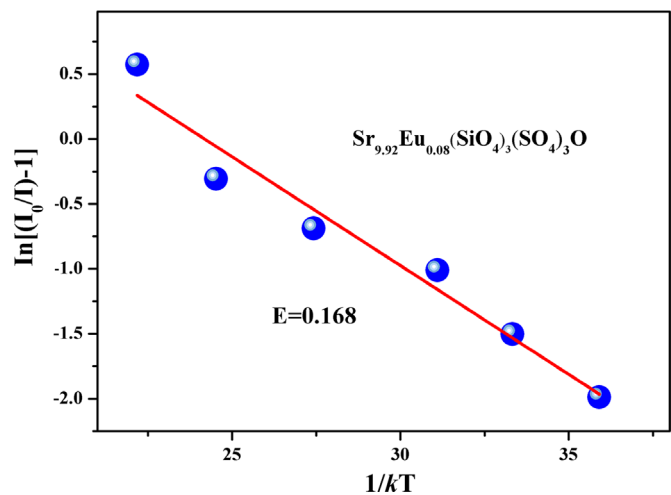
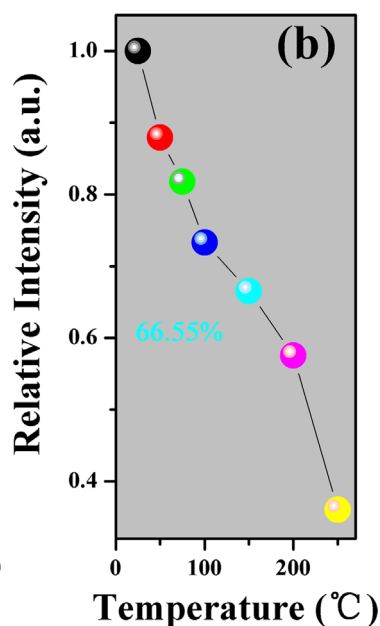


Fig. 7. $\ln[(I_0/I_T) - 1]$ vs. $1/kT$ activation energy graph for thermal quenching of $\text{Sr}_{9.92}(\text{SiO}_4)_3(\text{SO}_4)_3\text{O}:0.08\text{Eu}^{2+}$ phosphor.

$$I_T = \frac{I_0}{1 + c \exp\left(-\frac{E}{kT}\right)} \quad (4)$$

Where I_0 is the initial intensity, I_T is the intensity at a given temperature T , c is a constant, E is the activation energy for thermal quenching, and k is the Boltzmann's constant ($8.617 \times 10^{-5} \text{ eV K}^{-1}$). Based on the equation, the activation energy E can be calculated via a linear fitting of $\ln[(I_0/I) - 1]$ against $1/kT$, where a straight slope equals $-E$. Therefore, E was intended to be 0.168 eV for $\text{Sr}_{9.92}(\text{SiO}_4)_3(\text{SO}_4)_3\text{O}:0.08\text{Eu}^{2+}$ phosphor shown in Fig. 7.

CIE chromaticity coordinates (x, y) of the $\text{Sr}_{9.92}(\text{SiO}_4)_3(\text{SO}_4)_3\text{O}:0.08\text{Eu}^{2+}$ sample upon 396 nm excitation calculated through its PL spectrum and the digital image of the sample under 365 nm UV lamp excitation are shown in Fig. 8. The color coordinate is calculated to be (0.3246, 0.6243), and the phosphor shows intense green emission shown in the inset of Fig. 8. Therefore, this phosphor can be used as a green-emitting phosphor for n-UV w-LEDs.



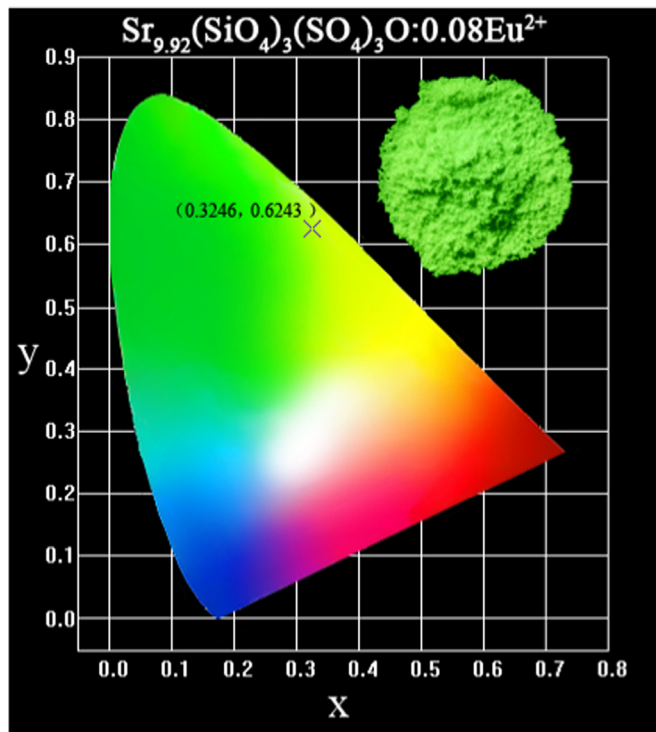


Fig. 8. Color coordinates of $\text{Sr}_{9.92}(\text{SiO}_4)_3(\text{SO}_4)_3\text{O}:0.08\text{Eu}^{2+}$ in the CIE chromaticity diagram, and the inset shows a digital photograph of the green-emitting phosphor excited at 365 nm.

4. Conclusions

In summary, a novel apatite structure phosphor SSSO:Eu²⁺ has been synthesized and investigated in this paper. The SSSO:Eu²⁺ phosphor exhibits a broad-band green emission at 538 nm under the excitation at 396 nm. In addition, SSSO:Eu²⁺ shows strong and broad absorption in the near UV regions and the optimum excitation band locates in the 250–525 nm region. Eu²⁺ can occupy both the Sr1 site with nine-coordination and Sr2 site with seven-coordination. Moreover, the dipole–dipole interactions results in the concentration quenching of Eu²⁺ in SSSO:Eu²⁺. The $\text{Sr}_{9.92}(\text{SiO}_4)_3(\text{SO}_4)_3\text{O}:0.08\text{Eu}^{2+}$ phosphor shows high thermal quenching temperature (66.55% of the initial intensity at 150 °C). The above results demonstrate the SSSO:Eu²⁺ phosphor can be used as green emitting phosphor in the w-LEDs.

Acknowledgments

This present work is supported by the National Natural Science Foundation of China (Grant no. 41172053).

References

- [1] Q.G. Xu, D.H. Xu, J.Y. Sun, Preparation and luminescence properties of orange-red $\text{Ba}_3\text{Y}(\text{PO}_4)_3:\text{Sm}^{3+}$ phosphors, Opt. Mater. 42 (2015) 210–214.
- [2] K. Li, J. Fan, X.Y. Mi, Y. Zhang, H.Z. Lian, M.M. Shang, J. Lin, Tunable-color luminescence via energy transfer in $\text{NaCa}_{13/18}\text{Mg}_{5/18}\text{PO}_4:\text{A}$ ($\text{A}=\text{Eu}^{2+}/\text{Tb}^{3+}/\text{Mn}^{2+}, \text{Dy}^{3+}$) phosphors for solid state lighting, Inorg. Chem. 53 (2014) 12141–12150.
- [3] Q.F. Guo, L.B. Liao, Z.G. Xia, Luminescence properties and energy transfer in $\text{La}_6\text{Ba}_4(\text{SiO}_4)_6\text{F}_2:\text{Ce}^{3+},\text{Tb}^{3+}$ phosphors, J. Lumin. 145 (2014) 65–70.
- [4] Q.F. Guo, L.B. Liao, L.F. Mei, H.K. Liu, Y. Hai, Color-tunable photoluminescence phosphors of Ce³⁺ and Tb³⁺ co-doped $\text{Sr}_2\text{La}_8(\text{SiO}_4)_6\text{O}_2$ for UV w-LEDs, J. Solid State Chem. 225 (2015) 149–154.
- [5] M.K. Kang, H.R. Jeong, Synthesis of $\text{Y}_3\text{Al}_5\text{O}_{12}:\text{Ce}^{3+}$ colloidal nanocrystals by pulsed laser ablation and their luminescent properties, J. Alloy. Compd. 576 (2013) 195–200.
- [6] C.H. Huang, T.M. Chen, W.R. Liu, Y.C. Chui, Y.T. Yeh, S.M. Jang, A single-phased emission-tunable phosphor $\text{Ca}_9\text{Y}(\text{PO}_4)_7:\text{Eu}^{2+},\text{Mn}^{2+}$ with efficient energy transfer for white-light-emitting diodes, ACS Appl. Mater. Interfaces 2 (2010) 259–264.
- [7] Z.H. Mao, Y.C. Zhu, Y. Wang, L. Gan, $\text{Ca}_2\text{SiO}_4:\text{Ln}$ ($\text{Ln}=\text{Ce}^{3+}, \text{Eu}^{2+}, \text{Sm}^{3+}$) tricolor emission phosphors and their application for near-UV white light-emitting diode, J. Mater. Sci. 49 (2014) 4439–4444.
- [8] Y.H. Song, H.P. You, M. Yang, Y.H. Zheng, K. Liu, G. Jia, Y.J. Huang, L.H. Zhang, H. J. Zhang, Facile synthesis and luminescence of $\text{Sr}_5(\text{PO}_4)_3\text{Cl}:\text{Eu}^{2+}$ nanorod bundles via a hydrothermal route, Inorg. Chem. 49 (2010) 1674–1678.
- [9] G. Bizarri, B. Moine, On the role of traps in the $\text{BaMgAl}_{10}\text{O}_{17}:\text{Eu}^{2+}$ fluorescence mechanisms, J. Lumin. 115 (2005) 53–61.
- [10] C.M. Huang, W.R. Liu, T.M. Chen, T.S. Chan, Y.T. Lai, Orangish-yellow-emitting $\text{Ca}_3\text{Si}_2\text{O}_7:\text{Eu}^{2+}$ phosphor for application in blue-light based warm-white LEDs, Dalton Trans. 43 (2014) 7917–7923.
- [11] K. Li, D.L. Geng, M.M. Shang, Y. Zhang, H.Z. Lian, J. Lin, Color-tunable luminescence and energy transfer properties of $\text{Ca}_6\text{Mg}(\text{PO}_4)_6\text{F}_2:\text{Eu}^{2+}, \text{Mn}^{2+}$ phosphors for UV-LEDs, J. Phys. Chem. C 118 (2014) 11026–11034.
- [12] C. Peng, G.G. Li, Z.Y. Hou, M.M. Shang, J. Lin, Electrospinning synthesis and luminescent properties of one-dimensional $\text{Ca}_2\text{Gd}_8(\text{SiO}_4)_6\text{O}:\text{Eu}^{3+}$ microfibers and microbelts, Mater. Chem. Phys. 136 (2012) 1008–1014.
- [13] G.G. Li, Y. Zhang, D.L. Geng, M.M. Shang, C. Peng, Z.Y. Cheng, J. Lin, Single-composition trichromatic white-emitting $\text{Ca}_4\text{Y}_6(\text{SiO}_4)_6\text{O}:\text{Ce}^{3+}/\text{Mn}^{2+}/\text{Tb}^{3+}$ phosphor: luminescence and energy transfer, ACS Appl. Mater. Interfaces 4 (2012) 296–305.
- [14] P.S. Thakre, S.C. Gedam, S.J. Dhoble, R.G. Atram, Luminescence investigations on sulfate apatite $\text{Na}_6(\text{SO}_4)_2\text{FCl}:\text{RE}$ ($\text{RE}=\text{Dy, Ce or Eu}$) phosphors, J. Lumin. 131 (2011) 2683–2689.
- [15] Bruker AXS, TOPAS V4: General profile and structure analysis software for powder diffraction data – user's manual, Bruker AXS, Karlsruhe, Germany, 2008.
- [16] K. Boughzala, S. Nasr, E.B. Salem, F. Kooli, K. Bouzouita, Structural and spectroscopic investigation of lanthanum-substituted strontium-oxybritholites, J. Chem. Sci. 121 (2009) 283–291.
- [17] R.D. Shannon, Revised effective ionic radii and systematic studies of interatomic distances in halides and chalcogenides, Acta Cryst. A 32 (1976) 751–767.
- [18] L.G. Van Uiter, An empirical relation fitting the position in energy of the lower d-band edge for Eu²⁺ or Ce³⁺ in various compounds, J. Lumin. 29 (1984) 1–9.
- [19] L.G. Van Uiter, Characterization of energy transfer interactions between rare earth ions, J. Electrochem. Soc. 114 (1967) 1048–1053.
- [20] G. Blasse, Energy transfer between inequivalent Eu²⁺ ions, J. Solid State Chem. 62 (1986) 207–211.
- [21] G. Blasse, Energy transfer in oxidic phosphors, Phys. Lett. A 28 (1968) 444–445.
- [22] W.Z. Lv, M.M. Jiao, Q. Zhao, B.Q. Shao, W. Lu, H.P. You, $\text{Ba}_{12}\text{Ca}_{0.7}\text{SiO}_4:\text{Eu}^{2+}, \text{Mn}^{2+}$: a promising single-phase, color-tunable phosphor for near-ultraviolet white-light-emitting diodes, Inorg. Chem. 53 (2014) 11007–11014.
- [23] X.G. Zhang, Y.B. Chen, L.Y. Zhou, Q. Pang, M.L. Gong, Synthesis of a broad-band excited and multicolor tunable phosphor $\text{Gd}_2\text{SiO}_5:\text{Ce}^{3+},\text{Tb}^{3+},\text{Eu}^{3+}$ for near-ultraviolet light-emitting diodes, Ind. Eng. Chem. Res. 53 (2014) 6694–6698.
- [24] R.J. Xie, N. Hirosaki, N. Kimura, K. Sakuma, M. Mitomo, 2-Phosphor-converted white light-emitting diodes using oxynitride/nitride phosphors, Appl. Phys. Lett. 90 (2007) 191101–191103.
- [25] C.L. Zhao, Z.G. Xia, S.X. Yu, Thermally stable luminescence and structure evolution of (K, Rb) BaPO₄:Eu²⁺ solid-solution phosphors, J. Mater. Chem. C 2 (2014) 6032–6039.
- [26] I. Baginskij, R.S. Liu, Significant improved luminescence intensity of Eu²⁺-doped $\text{Ca}_3\text{SiO}_4\text{Cl}_2$ Green phosphor for white leds synthesized through two-stage method, J. Electrochem. Soc. 156 (2009) 29–32.